University of Kentucky
UKnowledge

Chemistry Faculty Publications | Chemistry

5-17-2013

Topography-Guided Spreading and Drying of 6,13-bis(triisopropylsilylethynyl)-pentacene Solution on a Polymer Insulator for the Field-Effect Mobility Enhancement

Chang-Min Keum
Seoul National University, South Korea

Jin-Hyuk Bae
Kyungpook National University, South Korea

Min-Hoi Kim
Seoul National University, South Korea

Hea-Lim Park
Seoul National University, South Korea

Marcia M. Payne
University of Kentucky, marcia.payne@uky.edu

See next page for additional authors

Follow this and additional works at: https://uknowledge.uky.edu/chemistry_facpub

Right click to open a feedback form in a new tab to let us know how this document benefits you.

Part of the Chemistry Commons

Repository Citation

Keum, Chang-Min; Bae, Jin-Hyuk; Kim, Min-Hoi; Park, Hea-Lim; Payne, Marcia M.; Anthony, John E.; and Lee, Sin-Doo, "Topography-Guided Spreading and Drying of 6,13-bis(triisopropylsilylethynyl)-pentacene Solution on a Polymer Insulator for the Field-Effect Mobility Enhancement" (2013). *Chemistry Faculty Publications*. 27.
https://uknowledge.uky.edu/chemistry_facpub/27

This Article is brought to you for free and open access by the Chemistry at UKnowledge. It has been accepted for inclusion in Chemistry Faculty Publications by an authorized administrator of UKnowledge. For more information, please contact UKnowledge@lsv.uky.edu.

Authors
Chang-Min Keum, Jin-Hyuk Bae, Min-Hoi Kim, Hea-Lim Park, Marcia M. Payne, John E. Anthony, and Sin-Doo Lee

Topography-Guided Spreading and Drying of 6,13-bis(triisopropylsilylethynyl)-pentacene Solution on a Polymer Insulator for the Field-Effect Mobility Enhancement

Notes/Citation Information
Published in *Applied Physics Letters*, v. 102, article 193307, p. 1-5.

Copyright 2013 American Institute of Physics. This article may be downloaded for personal use only. Any other use requires prior permission of the author and the American Institute of Physics.

The following article appeared in *Applied Physics Letters*, v. 102, article 193307, p. 1-5 and may be found at http://dx.doi.org/10.1063/1.4807461.

Digital Object Identifier (DOI)
http://dx.doi.org/10.1063/1.4807461

This article is available at UKnowledge: https://uknowledge.uky.edu/chemistry_facpub/27

Topography-guided spreading and drying of 6,13-bis(triisopropylsilylethynyl)-pentacene solution on a polymer insulator for the field-effect mobility enhancement

Chang-Min Keum,[1] Jin-Hyuk Bae,[2] Min-Hoi Kim,[1] Hea-Lim Park,[1] Marcia M. Payne,[3] John E. Anthony,[3] and Sin-Doo Lee[1,a)]
[1]*School of Electrical Engineering, Seoul National University, Kwanak P.O. Box 34, Seoul 151-600, South Korea*
[2]*School of Electronics Engineering, Kyungpook National University, 1370 Sankyuk-dong, Bukgu, Daegu 702-701, South Korea*
[3]*Department of Chemistry, University of Kentucky, Lexington, Kentucky 40506-0055, USA*

(Received 9 April 2013; accepted 5 May 2013; published online 17 May 2013)

We report on the enhancement of the field-effect mobility of solution-processed 6,13-bis(triisopropylsilylethynyl)-pentacene (TIPS-pentacene) by unidirectional topography (UT) of an inkjet-printed polymer insulator. The UT leads to anisotropic spreading and drying of the TIPS-pentacene droplet and enables to spontaneously develop the ordered structures during the solvent evaporation. The mobility of the UT-dictated TIPS-pentacene film (0.202 ± 0.012 cm^2/Vs) is found to increase by more than a factor of two compared to that of the isotropic case (0.090 ± 0.032 cm^2/Vs). The structural arrangement of the TIPS-pentacene molecules in relation to the mobility enhancement is described within an anisotropic wetting formalism. Our UT-based approach to the mobility enhancement is easily applicable to different classes of soluble organic field-effect transistors by adjusting the geometrical parameters such as the height, the width, and the periodicity of the UT of an inkjet-printed insulator. © *2013 AIP Publishing LLC*. [http://dx.doi.org/10.1063/1.4807461]

Solution-processed organic field-effect transistors (OFETs) have been extensively investigated for flexible, large-area, and low-cost electronic applications[1–3] owing to the simplicity in fabrication by simple printing and/or roll-to-roll processing, for example, using inkjet printing.[4–6] Apart from the materials themselves being used, several issues such as the device architecture, the energy level alignment at organic semiconductor (OSC)-metal-insulator interfaces, and the charge transport should be tailored for developing high-performance OFETs. Of particular importance in solution-processing are the interfacial properties of an OSC solution in contact with the gate insulator since they play critical roles on the field-effect mobility,[7] the current leakage,[8] and the uniformity[9] of the OSC film in a fully dried state. In OSCs with π-orbital interactions between co-facially stacked molecules, improved chain ordering is known to significantly increase the mobility.[10,11] Especially, for soluble low-molecular OSCs such as 6,13-bis(triisopropylsilylethynyl) pentacene (TIPS-pentacene), the molecular order is induced by either dip coating,[12] solution-shearing,[13] or hollow pen writing.[14] The use of blended TIPS-pentacene with a photo-reactive polymer[15] is another method of producing the molecular order when the exposure of ultra-violet light is carried out during the solvent evaporation. From the viewpoint of the interfacial interactions, the physicochemical modification of the gate insulator surface can be achieved using a hydrophobic layer for the improvement of the crystallinity in the soluble OSC.[6,16] In this case, the hydrophobic layer is necessarily different from the gate insulator so that the dielectric properties of the gate insulator are inevitably altered. Therefore, a new approach taking into account the fluidic and volatile nature of the OSC solution should be explored for the mobility enhancement without sacrificing other electrical properties of the OFET.

In this work, we introduce a concept of the unidirectional topography (UT) of an inkjet-printed polymer insulator to produce anisotropic spreading and drying of the TIPS-pentacene droplet and to spontaneously develop the ordered structures over relatively large area during the solvent evaporation. The formation of ordered structures showing optical anisotropy in the solution-processed TIPS-pentacene film leads directly to the enhancement of the field-effect mobility. In contrast to the alignment of a liquid crystal, which is a highly viscous and non-volatile fluid, on a micro-grooved surface according to the elasticity argument,[17] the structural arrangement of the TIPS-pentacene molecules is most likely achieved through anisotropic wetting, spreading, and drying along the UT on the gate insulator produced by inkjet printing. The development of the structural order of the TIPS-pentacene molecules is described in terms of the anisotropic wetting phenomenon together with the directional flow during the solvent evaporation along the UT.

The construction of the UT of a polymer insulator by inkjet printing is schematically shown in Fig. 1(a). As shown in the figure, a series of the droplets of a polymer solution are printed in line such that the droplets are partially connected. As a basic element of the UT, a ridge structure with periodic arcs is naturally developed during the anisotropic solvent evaporation along the direction of inkjet printing. Note that the periodic arc boundary in the ridge is attributed to the coffee-ring effect,[18–20] which is commonly observed in a liquid droplet containing dispersed solids during the

a)Electronic mail: sidlee@plaza.snu.ac.kr

 © 2013 AIP Publishing LLC

This article is copyrighted as indicated in the article. Reuse of AIP content is subject to the terms at: http://scitation.aip.org/termsconditions. Downloaded to IP: 128.163.8.74 On: Wed, 21 Oct 2015 19:04:43

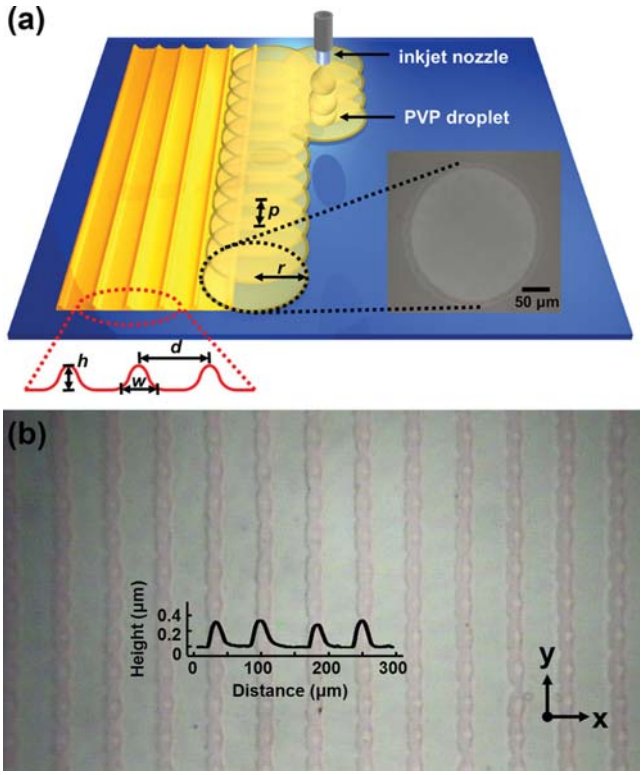

FIG. 1. (a) Schematic diagram showing the construction of UT of PVP on top of the uniform PVP insulator by inkjet printing. The radius of a single PVP droplet and the printing pitch are denoted by r and p, respectively. The width and the height of the ridge formed by a series of the droplets printed in line are w and h, respectively. The center-to-center distance between two adjacent ridges is d. The inset is the optical microscopic image of a single PVP droplet pattern showing the coffee-ring effect. (b) The optical microscopic image of PVP ridges constructed on the uniform PVP layer by inkjet printing and the geometrical profiles of several PVP ridges. The x-axis and y-axis are defined as the directions perpendicular and parallel to UT, respectively.

drying process. The inset in Fig. 1(a) shows the optical microscopic image of a single droplet pattern of poly(4-vinylphenol) (PVP) on the uniform PVP layer, where the coffee-ring effect is clearly seen. The geometrical factors such as the width (w) and the height (h) of the ridge depend primarily on the printing pitch (p) and the radius (r) of the droplet of the polymer solution. The center-to-center distance (d) between two adjacent ridges is simply given by the spatial interval in inkjet printing. A polymer dielectric material of PVP mixed with methylated poly(melamine-co-formaldehyde) (MMF) (100 wt. % of PVP) in propylene glycol methyl ether acetate (PGMEA) in 5 wt. % was used for producing the gate insulator with the ridge structures by inkjet printing. Inkjet printing was performed using a piezoelectric printer (UJ200, Unijet Co.), equipped with a nozzle having the orifice diameter of 50 μm (MJ-AT, MicroFab), at a frequency of 1 kHz in an asymmetric bipolar type wave form. The ridge structures of PVP were constructed on top of a uniform PVP layer, which was prepared on a glass substrate by spin-coating. The substrate was maintained at 60 °C during inkjet printing. For a single PVP droplet with the volume of 40 pl in solution, the average radius (r) on the uniform PVP layer was about 110 μm as shown in the inset of Fig. 1(a). The optical microscopic image of the PVP ridges constructed on the uniform PVP layer by inkjet printing was shown in Fig. 1(b). From the geometrical profiles of the PVP ridge measured using a surface profiler (alpha step 500, KLA-Tencor), it was found that $h = 350$ nm, $w = 30\,\mu$m, and $d = 55\,\mu$m. These parameters depend on the experimental conditions, such as the volume (or the radius) of the droplet, the printing pitch, the solvent evaporation rate, and the substrate temperature, together with the intrinsic properties of the substrate including the surface energy and the morphology. Note that in our case, the periodic ridges forming the UT were built up in the PVP-on-PVP configuration to eliminate any detrimental effect at an insulator-insulator interface.

We first examined the wetting behavior of water on two types of PVP insulator surfaces, one of which is spatially uniform and the other has the UT. The x-axis and the y-axis represent the direction perpendicular to the ridge and the direction parallel to the ridge, respectively, as shown in Fig. 1(b). The contact angle of water on a uniform PVP surface was circularly symmetric ($\theta_s = 75°$) as shown in Fig. 2(a). For the UT on the uniform PVP, as seen from Figs. 2(b) and 2(c), the contact angle was $\theta_\perp = 81°$ along the y-axis, while it was $\theta_\parallel = 70°$ along the x-axis according to the geometrical anisotropy of the UT. This is consistent with the anisotropic wetting phenomena of liquids on a large number of textured surfaces.[21–24] In Wenzel's model[25–27] for anisotropic wetting of a liquid on a textured surface, the relationship between the apparent angle θ_a and the intrinsic contact angle θ on a

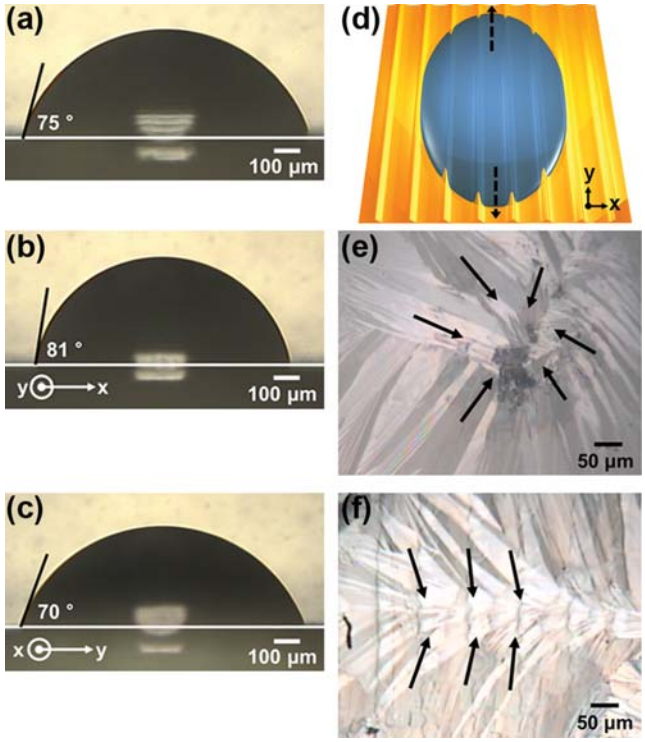

FIG. 2. The contact angles of water on (a) the uniform PVP insulator prepared by spin-coating (θ_s), (b) on PVP insulator with the UT measured along the y-axis ($\theta_\perp$), and (c) on PVP insulator with UT measured along the x-axis ($\theta_\parallel$). (d) The schematic illustration of an elongated TIPS-pentacene droplet formed on PVP insulator with UT by anisotropic wetting. The black dashed arrows indicate the directions of preferential spreading of the droplet along the ridges. The optical microscopic images of the TIPS-pentacene films prepared (e) on a uniform PVP film and (f) on PVP with UT. The radial domains on the uniform PVP and the elongated, bilateral domains along UT of PVP are indicated by black solid arrows.

This article is copyrighted as indicated in the article. Reuse of AIP content is subject to the terms at: http://scitation.aip.org/termsconditions. Downloaded to IP: 128.163.8.74 On: Wed, 21 Oct 2015 19:04:43

smooth surface can be expressed as $\cos\theta_a = k\cos\theta$, where k is a constant depending on the ratio of the effective surface area in contact with the liquid to the projected surface area. Moreover, it is well known that the geometrical anisotropy on the textured surface breaks the symmetry of the contact line at the liquid-solid boundary,[22] indicating that the liquid tends to spread along the ridges but is restricted in the direction perpendicular to the ridges. This means that the liquid droplet should be elongated along the ridge direction. In other words, using $\theta = 75°$, k was about 1.3 for $\theta_a = 70°$ and about 0.6 for $\theta_a = 81°$ in a first-order approximation, where the interfacial interactions are ignored.[22,23] Similarly, for the TIPS-pentacene solution, an elongated droplet is formed on the PVP insulator with the UT by anisotropic wetting as shown schematically in Fig. 2(d). The directional flow is then generated along the UT during the solvent evaporation, and the structural order of the TIPS-pentacene molecules is accordingly developed. In our study, a droplet of 1 μl of TIPS-pentacene dissolved in anisole in 1 wt. % was placed on the PVP insulator with the UT at room temperature and allowed for the solvent evaporation at 60 °C for 30 min. The optical microscopic image of the TIPS-pentacene film prepared on a uniform PVP film and that on the UT of the PVP is shown in Figs. 2(e) and 2(f), respectively. It is clear that in contrast to the random, radial domains (indicated by black arrows) observed on the uniform PVP insulator, the elongated, bilateral domains were developed along the UT of the PVP insulator as shown in Fig. 2(f).

In analyzing the structural order of the TIPS-pentacene molecules in terms of the optical anisotropy, the optical retardation measurements were carried out using a photoelastic modulator (PEM) (PEM90, Hinds Instruments), which has been commonly used for characterizing liquid crystals[28,29] and pentacenes,[30] as shown in Fig. 3(a). The PEM with a fused silica head was placed between two crossed polarizers that were oriented at ±45° with respect to the optic axis of the PEM head. A 633 nm-laser beam was incident normal to the TIPS-pentacene film sample. The signal fed into a lock-in amplifier (SR830, Stanford Research Systems) from a photodetector was monitored during rotation of the sample. Figure 3(b) shows the optical retardation values for the uniform PVP insulator (open circles) and those for the PVP insulator with the UT (filled circles) as a function of the azimuthal rotation angle (φ). In both cases, the PVP insulators were optically isotropic irrespective of the presence of the UT. However, when the TIPS-pentacene film was crystallized on the PVP insulator after the solvent evaporation, the optical anisotropy resulting from the molecular order was observed as shown in Figs. 3(c) and 3(d). Different color curves represent five different samples we studied. For the uniform PVP case, the magnitude of the optical anisotropy and the direction of the optic axis of the TIPS-pentacene film were quite different from sample to sample as shown in Fig. 3(c), while for the UT case, the optic axis was very well-defined along the UT and the magnitude was fairly constant as shown in Fig. 3(d). The average value of the retardation maxima of the five samples was found to be 0.279 ± 0.072 for the uniform PVP case and 0.366 ± 0.037 for the UT case. This indicates that the UT of the PVP insulator indeed increases the degree of the molecular order and the crystallinity of the TIPS-pentacene film by the directional flow during the solvent evaporation.

We now investigate the electrical properties of the TIPS-pentacene OFETs with two types of PVP insulators, one with no UT and the other with the UT, in a bottom-gate, top-contact configuration as illustrated in Fig. 4(a). The gate electrode was prepared using 120 nm-thick-indium-tin-oxide, and the source and drain electrodes were gold (60 nm). The channel was produced along a direction either perpendicular or parallel to the UT of the PVP insulator. The channel length (L) and the channel width (W) were 50 μm and 1000 μm, respectively, defined by a metal shadow mask

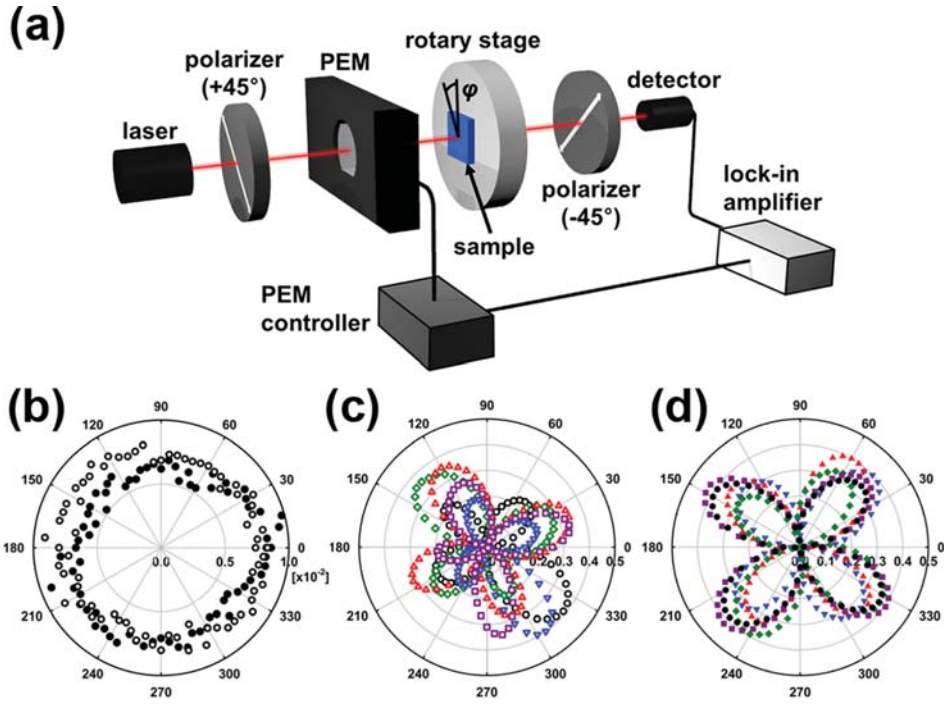

FIG. 3. (a) The experimental setup for the measurements of the optical anisotropy. The optical retardation values for (b) the uniform PVP (open circles) and PVP with UT (filled circles), (c) TIPS-pentacene film on the uniform PVP, and (d) TIPS-pentacene film on PVP with UT. Different colors represent five different samples.

This article is copyrighted as indicated in the article. Reuse of AIP content is subject to the terms at: http://scitation.aip.org/termsconditions. Downloaded to IP: 128.163.8.74 On: Wed, 21 Oct 2015 19:04:43

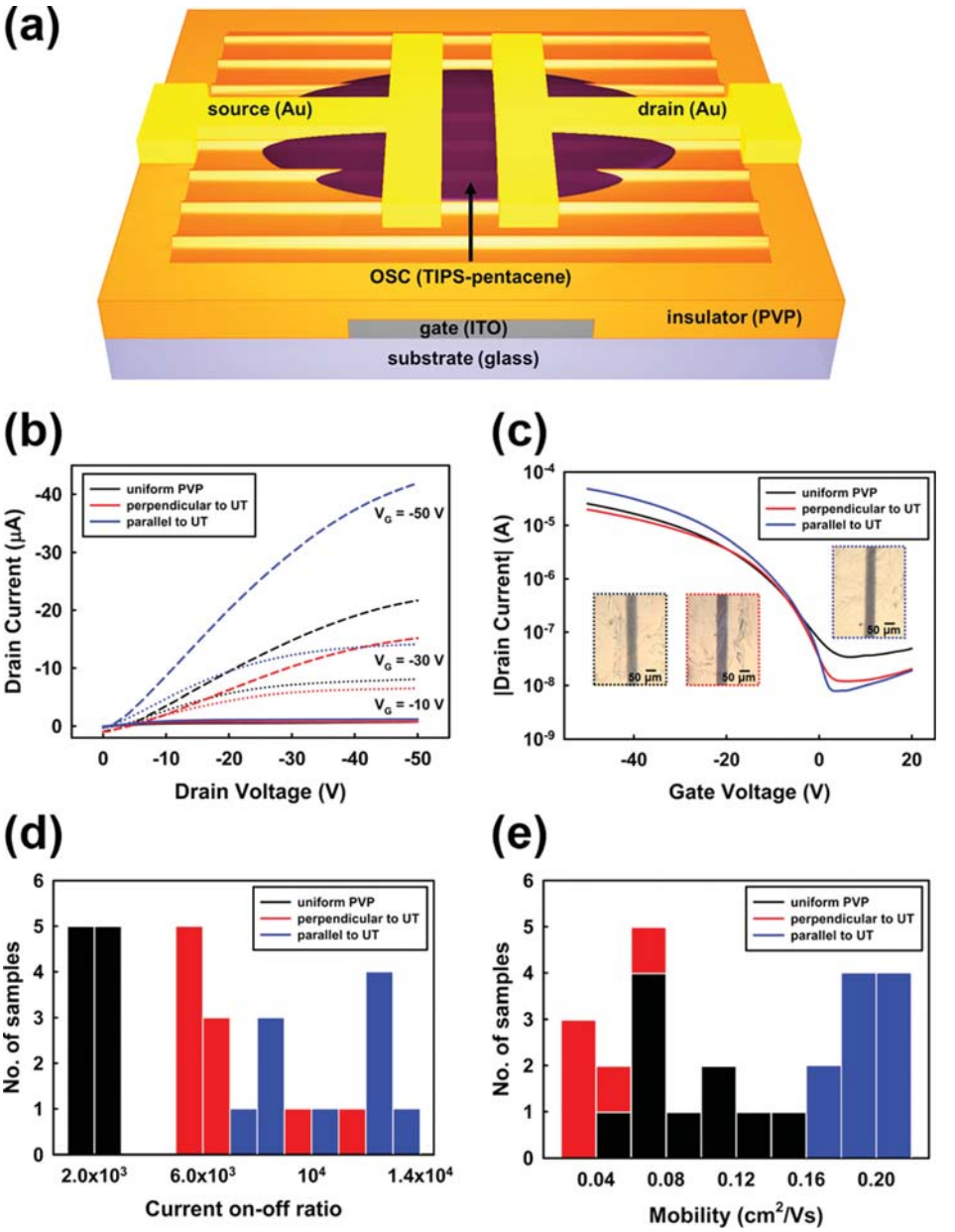

FIG. 4. (a) Schematic diagram showing a TIPS-pentacene OFET on PVP insulator with UT in a bottom-gate, top-contact configuration. (b) The output characteristics as a function of drain voltage for the gate voltages of −10 V (solid lines), −30 V (dotted lines), and −50 V (dashed lines) for three OFETs on the uniform PVP (black lines), on PVP with UT perpendicular to the channel (red lines), and on PVP with UT parallel to the channel (blue lines). (c) The transfer curves for the three cases as a function of the gate voltage at the drain voltage of −50 V. The insets are the optical microscopic images of the channel regions for the three cases. Histograms showing the distribution of (d) the current on-off ratio values and (e) that of the mobility values for the three cases.

during thermal evaporation. For the PVP insulator with the UT, there are two different channel geometries in the directions perpendicular and parallel to the UT. The electrical characteristics were measured using a semiconductor parameter analyzer (HP 4155 A, Agilent Technologies). Figure 4(b) shows the output characteristics of three OFETs, the first on the uniform PVP, the second on the UT perpendicular to the channel, and the third on the UT parallel to the channel, as a function of drain voltage for the gate voltages of −10 V, −30 V, and −50 V. The difference in the saturated drain current between the uniform PVP case and the UT case along the channel increases with increasing the drain voltage for given gate voltage. Relative to the uniform PVP case, the saturated drain current for the channel parallel to the UT was increased by more than twofold but that for the channel perpendicular to the UT was decreased by a factor of about one half.

The transfer characteristics for the three cases were shown as a function of the gate voltage at the drain voltage of −50 V in Fig. 4(c). The insets are the optical microscopic images of the channel regions for the three cases. It is clear that for the channel parallel to the UT, the uniformity of the TIPS-pentacene film was significantly improved, and the magnitude of the drain current was much enhanced. Another point is that the UT results in the reduction of the off-current irrespective of the channel geometry as shown in Fig. 4(c). This may be attributed to the role of the UT to screen out the vertical charge flow generated from the gate electrode, which is consistent with previous work.[8] Thus, the current on-off ratio was substantially increased (about 10^4) for the case of UT parallel to the channel. Figure 4(d) shows the distribution of the current on-off ratio values of ten OFETs fabricated in different batches for the three cases.

From the transfer characteristic curves in Fig. 4(c), the field-effect mobility of each OFET can be extracted from the slope of the square root of the saturated drain current (I_{Dsat}) as a function of the gate voltage (V_G) in the following equation:[31]

This article is copyrighted as indicated in the article. Reuse of AIP content is subject to the terms at: http://scitation.aip.org/termsconditions. Downloaded to IP: 128.163.8.74 On: Wed, 21 Oct 2015 19:04:43

$$\mu_{sat} = \frac{2L}{WC_i}\left(\frac{\partial\sqrt{I_{D\,sat}}}{\partial V_G}\right)^2, \quad (1)$$

where C_i denotes the capacitance per unit area of the gate insulator and μ_{sat} the mobility in the saturation region. The capacitance in a metal-insulator-metal structure as a function of the voltage was measured using a semiconductor analyzer (4200-SCS, Keithley instruments, Inc.). The measured values of C_i for the uniform PVP and the PVP with the UT were about 4.9 nF/cm^2 and 3.9 nF/cm^2, respectively. The average mobility values measured for the three cases, i.e., the channel on the uniform PVP (μ_s), the channel parallel to the UT on the PVP ($\mu_{\parallel}$), and the channel perpendicular to the UT on the PVP ($\mu_{\perp}$), over ten different samples were $\mu_s = 0.090 \pm 0.032$, $\mu_{\parallel} = 0.202 \pm 0.012$, and $\mu_{\perp} = 0.052 \pm 0.014\,\mathrm{cm}^2/\mathrm{Vs}$. The mobility was enhanced by 2.2 along the direction of the UT but decreased by 0.6 in the direction perpendicular to the UT. The distribution of the mobility values for the three cases is shown in Fig. 4(e).

In summary, we demonstrated the concept of UT for the enhancement of the field-effect mobility of solution-processed TIPS-pentacene on an inkjet-printed polymer insulator. The underlying mechanism for the ordered structures of TIPS-pentacene arises from the anisotropic wetting, spreading, and drying phenomenon guided by the UT during the solvent evaporation. The mobility of the UT-dictated TIPS-pentacene film was found to increase by more than two compared to that of the isotropic case. Moreover, the off-current was much reduced and the current on-off ratio was significantly increased by screening out the vertical charge flow generated from the gate electrode. Our UT-based approach will serve as a firm basis for developing diverse solution-processed organic devices including the OFETs and inverters provided that the geometrical parameters of the UT are properly designed for specific applications.

This work was supported in part by the National Research Foundation of Korea under the Ministry of Education, Science and Technology of Korea through the Grant No. 2011-0028422. One of the authors (J.E.A.) acknowledges the support from the US Office of Naval Research.

[1]H. Yan, Z. Chen, Y. Zheng, C. Newman, J. R. Quinn, F. Dotz, M. Kastler, and A. Facchetti, Nature **457**, 679 (2009).
[2]M. Mas-Torrent and C. Rovira, Chem. Soc. Rev. **37**, 827 (2008).
[3]S. Allard, M. Forster, B. Souharce, H. Thiem, and U. Scherf, Angew. Chem., Int. Ed. Engl. **47**, 4070 (2008).
[4]H. Sirringhaus, T. Kawase, R. H. Friend, T. Shimoda, M. Inbasekaran, W. Wu, and E. P. Woo, Science **290**, 2123 (2000).
[5]T. Sekitani, Y. Noguchi, U. Zschieschang, H. Klauk, and T. Someya, Proc. Natl. Acad. Sci. U.S.A. **105**, 4976 (2008).
[6]Y. H. Kim, B. Yoo, J. E. Anthony, and S. K. Park, Adv. Mater. **24**, 497 (2012).
[7]P. Liu, Y. Wu, Y. Li, B. S. Ong, and S. Zhu, J. Am. Chem. Soc. **128**, 4554 (2006).
[8]C.-M. Keum, J.-H. Bae, M.-H. Kim, W. Choi, and S.-D. Lee, Org. Electron. **13**, 778 (2012).
[9]Z. R. He, K. Xiao, W. Durant, D. K. Hensley, J. E. Anthony, K. L. Hong, S. M. Kilbey, J. H. Chen, and D. W. Li, Adv. Funct. Mater. **21**, 3617 (2011).
[10]J. E. Anthony, J. S. Brooks, D. L. Eaton, and S. R. Parkin, J. Am. Chem. Soc. **123**, 9482 (2001).
[11]S. C. Mannsfeld, M. L. Tang, and Z. Bao, Adv. Mater. **23**, 127 (2011).
[12]C. W. Sele, B. K. C. Kjellander, B. Niesen, M. J. Thornton, J. B. P. H. van der Putten, K. Myny, H. J. Wondergem, A. Moser, R. Resel, A. J. J. M. van Breemen, N. van Aerle, P. Heremans, J. E. Anthony, and G. H. Gelinck, Adv. Mater. **21**, 4926 (2009).
[13]G. Giri, E. Verploegen, S. C. Mannsfeld, S. Atahan-Evrenk, H. Kim do, S. Y. Lee, H. A. Becerril, A. Aspuru-Guzik, M. F. Toney, and Z. Bao, Nature **480**, 504 (2011).
[14]R. L. Headrick, S. Wo, F. Sansoz, and J. E. Anthony, Appl. Phys. Lett. **92**, 063302 (2008).
[15]J. Park, C.-M. Keum, J.-H. Kim, S.-D. Lee, M. Payne, M. Petty, J. E. Anthony, and J.-H. Bae, Appl. Phys. Lett. **102**, 013306 (2013).
[16]A. L. Briseno, S. C. Mannsfeld, M. M. Ling, S. Liu, R. J. Tseng, C. Reese, M. E. Roberts, Y. Yang, F. Wudl, and Z. Bao, Nature **444**, 913 (2006).
[17]D. W. Berreman, Phys. Rev. Lett. **28**, 1683 (1972).
[18]R. D. Deegan, O. Bakajin, T. F. Dupont, G. Huber, S. R. Nagel, and T. A. Witten, Nature **389**, 827 (1997).
[19]H. Hu and R. G. Larson, J. Phys. Chem. B **110**, 7090 (2006).
[20]D. Soltman and V. Subramanian, Langmuir **24**, 2224 (2008).
[21]M. Gleiche, L. F. Chi, and H. Fuchs, Nature **403**, 173 (2000).
[22]J. Y. Chung, J. P. Youngblood, and C. M. Stafford, Soft Matter **3**, 1163 (2007).
[23]W. Choi, A. Tuteja, J. M. Mabry, R. E. Cohen, and G. H. McKinley, J. Colloid Interface Sci. **339**, 208 (2009).
[24]S. G. Lee, H. S. Lim, D. Y. Lee, D. Kwak, and K. Cho, Adv. Funct. Mater. **23**, 547 (2013).
[25]R. N. Wenzel, Ind. Eng. Chem. **28**, 988 (1936).
[26]A. Lafuma and D. Quere, Nature Mater. **2**, 457 (2003).
[27]X. J. Feng and L. Jiang, Adv. Mater. **18**, 3063 (2006).
[28]J.-H. Kim, S. Kumar, and S.-D. Lee, Phys. Rev. E **57**, 5644 (1998).
[29]J.-H. Lee, C.-J. Yu, and S.-D. Lee, Mol. Cryst. Liq. Cryst. **321**, 317 (1998).
[30]C.-J. Yu, J.-H. Bae, C.-M. Keum, and S.-D. Lee, Curr. Appl. Phys. **10**, 64 (2010).
[31]R. Bourguiga, M. Mahdouani, S. Mansouri, and G. Horowitz, Eur. Phys. J: Appl. Phys. **39**, 7 (2007).

This article is copyrighted as indicated in the article. Reuse of AIP content is subject to the terms at: http://scitation.aip.org/termsconditions. Downloaded to IP: 128.163.8.74 On: Wed, 21 Oct 2015 19:04:43